Microscopic structures of MgO barrier layers in single-crystal Fe/MgO/Fe magnetic tunnel junctions showing giant tunneling magnetoresistance

doi: 10.1063/1.2213953

Microscopic structures of MgO barrier layers in single-crystal Fe/MgO/Fe magnetic tunnel junctions showing giant tunneling magnetoresistance

M. Mizuguchi[a] and Y. Suzuki
Department of Materials Engineering Science, Graduate School of Engineering Science, Osaka University, Toyonaka, Osaka 560-8531, Japan and Core Research for Evolutional Science and Technology (CREST), Japan Science and Technology Agency, Kawaguchi, Saitama 332-0012, Japan

T. Nagahama and S. Yuasa
NanoElectronics Research Institute, National Institute of Advanced Industrial Science and Technology (AIST), Tsukuba, Ibaraki 305-8568, Japan and Core Research for Evolutional Science and Technology (CREST), Japan Science and Technology Agency, Kawaguchi, Saitama 332-0012, Japan

(Received 24 February 2006; accepted 2 May 2006; published online 19 June 2006)

The microscopic structures of MgO(001) barrier layers in magnetic tunnel junctions showing giant tunneling magnetoresistance were characterized by *in situ* scanning tunneling microscopy. The MgO thin films formed exceedingly flat surfaces, and their terraces were made even flatter by annealing after deposition. This flattening of MgO surfaces apparently promotes coherent transport of electrons, which should enhance the tunneling magnetoresistance ratio. Local tunneling spectroscopy revealed that an annealed MgO layer has a critical thickness between 3 and 5 ML (monolayer), and a continuous film without pinholes can be formed over the thickness. © *2006 American Institute of Physics*. [DOI: 10.1063/1.2213953]

The physics of the tunneling magnetoresistance (TMR) effect and its application to devices have been energetically studied since its discovery a decade ago.[1,2] A greatly desired point has been to obtain magnetic tunnel junctions (MTJs) with sufficiently high TMR ratios even at room temperature. Two methods, in particular, have been proposed for enhancing the TMR ratio: (1) use high spin-polarized ferromagnets such as half-metals for the electrodes[3] and (2) use epitaxial magnesium oxide (MgO) layers as tunnel barriers.[4,5] There have been several reports on the fabrication and improvement of performance of MTJs with epitaxial MgO barriers,[6–10] and giant TMR ratios (larger than 150%) have been obtained even at room temperature by using high-quality MgO(001) barriers and/or suitable ferromagnetic electrodes.[11–17]

A highly oriented MgO(001) barrier yields a large TMR ratio, and it is supposed that the ratio is very sensitive to the structure of the interface between the barrier and electrodes.[18] It is therefore essential to characterize MgO(001) surface structures in real space to clarify the mechanism of the giant TMR effect. While topological scanning tunneling microscope (STM) images of MgO thin films have been obtained,[6,7,19–22] there have been no reports of MTJs with giant TMR ratios. Moreover, MTJs with low impedance are particularly essential for magnetic sensor applications, such as the read heads of hard disk drives. The characterization of MgO barriers with a few monolayer (ML) thicknesses is thus a pressing issue.

In this letter, we describe our characterization of the microscopic structures of MgO(001) barriers in a single-crystal Fe/MgO/Fe MTJ. *In situ* STM observations were performed to clarify the relationship between the structures and the magnetotransport properties. We used a system in which we can carry out deposition and STM observations alternately.[23] The annealing effects and thickness dependence of MgO barriers were also investigated in detail.

Single-crystal MgO(001) substrates were cut into 6 $\times 10$ mm^2 pieces. Subsequent partial deposition of the contact electrodes enabled STM observation. Layers of Fe and MgO were grown in a molecular-beam epitaxy (MBE) chamber by electron-beam evaporation of source materials. Their thicknesses were estimated using quartz crystal microbalances within the chamber. Microscopic studies of their surfaces were performed at RT in a STM chamber linked to the MBE chamber under an ultrahigh vacuum (UHV). Topological images were acquired using a tungsten-scanning tip in constant current mode. (The bias voltage means the potential of the sample against the tip hereafter.) The electronic structures of the MgO barriers were investigated using scanning tunneling spectroscopy (STS) method at several points on the barriers.

First, a MgO buffer layer with a thickness of 20 nm was grown at 638 K on a prebaked MgO(001) substrate in order to obtain good crystallinity. Then, a 50-nm-thick Fe(001) bottom electrode was epitaxially grown at RT on the buffer layer. This electrode layer was annealed at 573 K for 20 min in UHV to promote flattening of the surface. Epitaxial growth was confirmed by observation of a reflection high-energy diffraction pattern with very sharp streaks. The Fe layer was observed to have considerably flat surface structures with roundish step edges, as shown in Fig. 1(a). This film consists of three or four Fe atomic planes and terraces with widths ranging from 30 to 100 nm. A line-scan profile at the location indicated by the dotted line in Fig. 1(a) revealed step heights of 0.14 nm, corresponding exactly to the atomic monolayer of Fe(001) [Fig. 1(b)]. A few terraces can be seen sloping from the horizontal plane. It is conceivable that the slopes originate from the screw dislocations of the Fe. This Fe surface structure differs completely from that grown on a Au(001) buffer layer, where rectangular terrace structures could be seen.[23]

[a]Author to whom correspondence should be addressed; electronic mail: mizuguchi@mp.es.osaka-u.ac.jp

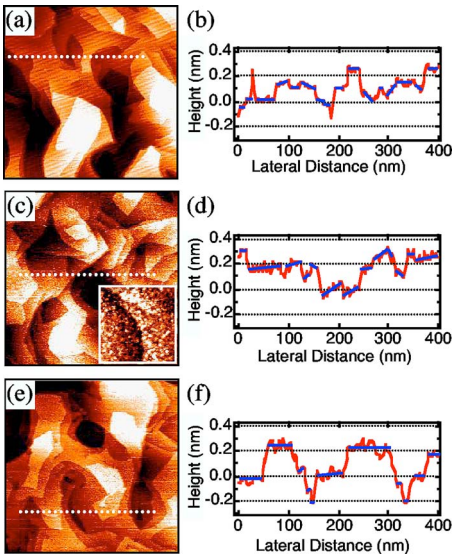

FIG. 1. (Color online) (a) 500×500 nm^2 STM image of a 50-nm-thick Fe layer grown on top of a 20-nm-thick MgO buffer layer (0.1 V, 0.3 nA). (b) Line-scan profile taken at location shown by the dotted line in (a). The solid lines are guides for the eyes. (c) 500×500 nm^2 STM image of 0.63-nm-thick MgO layer grown on top of Fe layer (1.5 V, 2.0 nA). The inset shows 50×50 nm^2 zoom in. (d) Line-scan profile taken at location shown by the dotted line in (c). The solid lines are guides for the eyes. (e) 500×500 nm^2 STM image of a 0.63-nm-thick MgO layer after annealing at 573 K for 30 min in UHV (1.0 V, 2.0 nA). (f) Line-scan profile taken at location shown by the dotted line in (e). The solid lines are guides for the eyes.

Epitaxial MgO barrier layers with various thicknesses were grown at RT on the Fe layer at a deposition rate of 0.01 nm/s. Figure 1(c) shows a topographic image of a MgO(001) layer with a thickness of 0.63 nm. Fundamentally, typical structures of the steps and terraces observed for the Fe (001) were also found in the MgO surface. Most of the step edges had step heights of about 0.14 nm, as shown in Fig. 1(d), which means that almost all parts of the MgO layer grew very flatly on the Fe surface structure, exactly like a *replica* of Fe. Sloped terraces were also found on the MgO barrier layer. One can see from the magnified image in Fig. 1(c) that minute clusters, several nanometers in size, were scattered over the surface, and this could be observed reproducibly. The existence of these clusters on MgO has previously been reported by other groups.[6,7] It is possible that these clusters are oxygen adsorbed before annealing,[13] although this is not very clear at the present stage.

We also investigated the effects of annealing the MgO barrier layers. The layers were annealed at 573 K for 30 min in UHV. After annealing, a considerable change in the surface topology was observed for the MgO barrier with a thickness of 0.63 nm, as shown in Fig. 1(e). Connections between adjacent terraces were clearly confirmed. Consequently, the terrace area increased in size on average, and terraces with widths of 50–100 nm were mainly observed. We should also note that the morphology of the terraces was improved, and surface flattening was achieved, as shown by the line profile in Fig. 1(f). Most estimated step heights were about 0.2 nm, which is very close to the thickness of one atomic layer of MgO(001) (0.21 nm). This increase in step height was probably due to recrystallization of the MgO layers and/or migration of the steps due to annealing, resulting in the partial appearance of the MgO step itself.

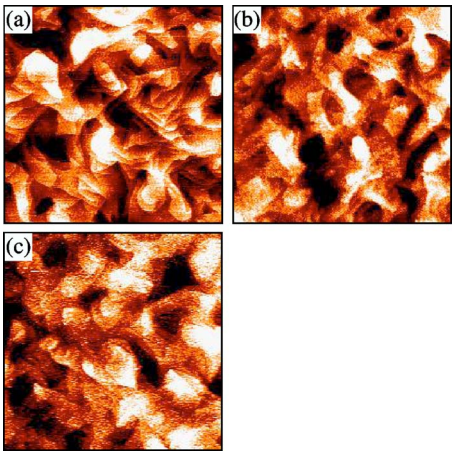

FIG. 2. (Color online) 1000×1000 nm^2 STM images of *as depo* MgO layers grown on top of Fe layer: (a) 0.63-nm-thick MgO layer (1.5 V, 2.0 nA), (b) 1.05-nm-thick MgO layer (2.0 V, 1.0 nA), and (c) 2.00-nm-thick MgO layer (5.0 V, 0.25 nA).

We investigated how the surface morphology changes with the thickness of the MgO barrier layer. Figure 2 shows the STM images of MgO surfaces with three different thicknesses (0.63, 1.05, and 2.00 nm) taken before annealing. Narrow terraces were observed for 0.63 nm [Fig. 2(a)] but not for 1.05 nm [Fig. 2(b)]. Large terraces with round step edges were observed for 2.0 nm [Fig. 2(c)]. The areas of the terraces generally increased with the thickness. As for the epitaxial MTJs with MgO barriers we studied, increasing the barrier thickness leads to an increase of the MR ratio,[13] corresponding to the increase of terrace areas observed here. The line scans related that the step heights for the 0.63-nm-thick MgO were mostly about 0.14 nm whereas those for the 1.05- and 2.00-nm-thick MgO were mostly about 0.2 nm in spite of surfaces before the annealing.[24]

Tunneling current as a function of bias voltage was monitored at several local points on the MgO barriers after annealing at 573 K for 30 min in UHV. Figure 3 shows the averaged *I-V* curves at the top terrace points (typically indicated by circles in the inset) and at the bottom terraces (indicated by crosses).[25] One can see a clear difference between the two curves for the 0.63-nm-thick barrier, as shown in Fig. 3(a). A distinct nonlinear line was obtained at the top points whereas the nonlinearity weakened at the bottom points. This indicates the existence of local holes in the barrier at the low points, meaning that this barrier (3 ML MgO) was an *imperfect* barrier. On the other hand, the spectra for the 1.05 nm barrier showed that the line shapes were similar between the top and bottom points, as shown in Fig. 3(b). This barrier (5 ML MgO) had a distinct band gap of approximately 2 eV even at bottom points, though the gaps were narrower than those previously reported.[7] This barrier can thus be considered *perfect*. The current asymmetry we observed is typical for the spectra of a perfect barrier.

The exceedingly flat surfaces with step and terrace structures of the MgO barriers may be the origin of the giant TMR effect, which should be caused by the coherent tunneling of electrons. The annealing after MgO barrier growth resulted in parallel terraces, as shown in Figs. 1(e) and 1(f), though it is unknown whether the Fe underlayer or the MgO layer itself migrated. We speculate that the flattening of terraces and the expansion of terrace areas lead to the reduction of electron scattering at the interface between MgO and Fe,

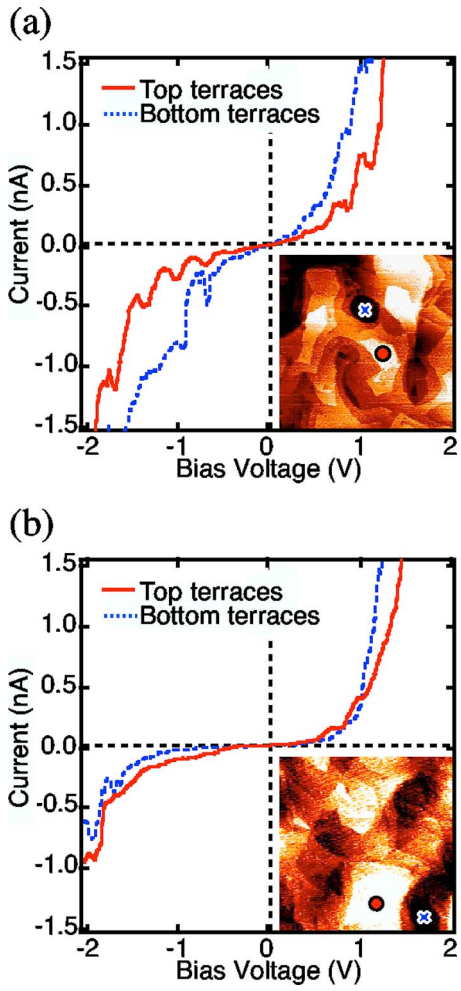

FIG. 3. (Color online) Averaged *I-V* curves measured at top terraces and at bottom terraces of (a) 0.63-nm-thick and (b) 1.05-nm-thick MgO layers. Common points were set at 1.5 V and 2.0 nA. Both layers were annealed at 573 K for 30 min in UHV. The insets show 500×500 nm^2 STM images of the two MgO surfaces. The positions indicated by circles and crosses typically show measured points for top and bottom terraces, respectively.

resulting in the coherent transport of electrons.

Our identification of pinholes in the barrier when the MgO thickness was 0.63 nm is not surprising because some parts of the Fe surface should not be covered with MgO because annealing mostly created MgO terraces with a step height of 0.21 nm. The MR ratio with this thickness was relatively low even after annealing, and the existence of the pinholes indicates that the transport process of a MTJ with a thin barrier cannot be explained by common TMR transport. Our finding that MgO with a thickness of 1.05 nm formed a continuous film even after annealing can be explained by the existence of a critical thickness between 0.63 (3 ML) and 1.05 nm (5 ML) where annealed MgO forms a continuous film.[26] A drastic increase in the MR ratio by annealing has been reported for MgO thicker than this critical thickness.[13] It is possible that not only the reduction of the dislocation density but the improvement of surface morphology by annealing resulted in the enhancement of the MR ratio.

In summary, we performed *in situ* STM observations of MgO(001) barriers with a thickness of a few monolayers in a single-crystal Fe/MgO/Fe MTJ. MgO layers with a thickness of 0.63 nm formed surface structures similar to those of the Fe underlayer, exactly like its replica, and annealing converted them into different structures with even flatter terraces. The areas of the terrace portions generally increased with the MgO thickness in the range of 0.63–2.00 nm, corresponding to the increase in the TMR ratio. STS investigation revealed that a 3 ML MgO layer after annealing forms an imperfect barrier with pinholes whereas a 5 ML MgO layer forms a continuous barrier. The relationship between the microscopic structures and the giant TMR ratios of MgO-based MTJs has thus been clarified.

The authors are grateful to M. Yamamoto of AIST for assisting with the experiments. This study was partly supported by Research and Development of Nanodevices for Practical Utilization of Nanotechnology (Nanotech Challenge Project) of New Energy and Industrial Technology Development Organization (NEDO). This work was partly supported by The 21st Century COE Program (G18) of the Japan Society for the Promotion of Science.

[1] J. S. Moodera, L. R. Kinder, T. M. Wong, and R. Meservey, Phys. Rev. Lett. **74**, 3273 (1995).
[2] T. Miyazaki and N. Tezuka, J. Magn. Magn. Mater. **139**, L231 (1995).
[3] M. Julliere, Phys. Lett. **54A**, 225 (1975).
[4] W. H. Butler, X.-G. Zhang, T. C. Schulthess, and J. M. MacLaren, Phys. Rev. B **63**, 054416 (2001).
[5] J. Mathon and A. Umersky, Phys. Rev. B **63**, 220403 (2001).
[6] W. Wulfhekel, M. Klaua, D. Ullmann, F. Zavaliche, J. Kirschner, R. Urban, T. Monchesky, and B. Heinrich, Appl. Phys. Lett. **78**, 509 (2001).
[7] M. Klaua, D. Ullmann, J. Barthel, W. Wulfhekel, J. Kirschner, R. Urban, T. L. Monchesky, A. Enders, J. F. Cochran, and B. Heinrich, Phys. Rev. B **64**, 134411 (2001).
[8] M. Bowen, V. Cros, F. Petroff, A. Fert, C. Martínez Boubeta, J. L. Costa-Krämer, J. V. Anguita, A. Cebollada, F. Briones, J. M. de Teresa, L. Morellón, M. R. Ibarra, F. Güell, F. Peiró, and A. Cornet, Appl. Phys. Lett. **79**, 1655 (2001).
[9] S. Mitani, T. Moriyama, and K. Takanashi, J. Appl. Phys. **93**, 8041 (2003).
[10] J. Faure-Vincent, C. Tiusan, E. Jouguelet, F. Canet, M. Sajieddine, C. Bellouard, E. Popova, M. Hehn, F. Montaigne, and A. Schuhl, Appl. Phys. Lett. **82**, 4507 (2003).
[11] S. Yuasa, A. Fukushima, T. Nagahama, K. Ando, and Y. Suzuki, Jpn. J. Appl. Phys., Part 2 **43**, L588 (2004).
[12] S. S. P. Parkin, C. Kaiser, A. Panchula, P. M. Rice, B. Hughes, M. Samant, and S. H. Yang, Nat. Mater. **3**, 862 (2004).
[13] S. Yuasa, T. Nagahama, A. Fukushima, Y. Suzuki, and K. Ando, Nat. Mater. **3**, 868 (2004).
[14] D. D. Djayaprawira, K. Tsunekawa, M. Nagai, H. Maehara, S. Yamagata, N. Watanabe, S. Yuasa, Y. Suzuki, and K. Ando, Appl. Phys. Lett. **86**, 092502 (2005).
[15] S. Yuasa, T. Katayama, T. Nagahama, A. Fukushima, H. Kubota, Y. Suzuki, and K. Ando, Appl. Phys. Lett. **87**, 222508 (2005).
[16] J. Hayakawa, S. Ikeda, F. Matsukura, H. Takahashi, and H. Ohno, Jpn. J. Appl. Phys., Part 2 **44**, L587 (2005).
[17] S. Ikeda, J. Hayakawa, Y. M. Lee, R. Sasaki, T. Meguro, F. Matsukura, and H. Ohno, Jpn. J. Appl. Phys., Part 2 **44**, L1442 (2005).
[18] C. Tiusan, M. Sicot, M. Hehn, C. Belouard, S. Andrieu, F. Montaigne, and A. Schuhl, Appl. Phys. Lett. **88**, 062512 (2006).
[19] S. Schintke, S. Messerli, M. Pivetta, F. Patthey, L. Libioulle, M. Stengel, A. De Vita, and W.-D. Schneider, Phys. Rev. Lett. **87**, 276801 (2001).
[20] S. Valeri, S. Altieri, U. del Pennino, A. di Bona, P. Luches, and A. Rota, Phys. Rev. B **65**, 245410 (2002).
[21] A. Subagyo, H. Oka, G. Eilers, K. Sueoka, and K. Mukasa, Jpn. J. Appl. Phys., Part 1 **39**, 3777 (2000).
[22] F. Ernult, K. Yamane, S. Mitani, K. Yakushiji, K. Takanashi, Y. K. Takahashi, and K. Hono, Appl. Phys. Lett. **84**, 3106 (2004).
[23] M. Mizuguchi, Y. Suzuki, T. Nagahama, and S. Yuasa, Appl. Phys. Lett. **87**, 171909 (2005).
[24] A few steps for the 1.05- and 2.00-nm-thick MgO had a height of 0.4 nm, indicating step bunching.
[25] More than ten curves were measured at different points for each case.
[26] The critical thickness of Al–O formed by natural oxidation is between 2 and 3 ML of aluminum.